

Volume diffusion of cobalt in tungsten single crystals

S. M. Klotsman, S. V. Osetrov, and A. N. Timofeev

Diffusion Phenomena Department, Institute of Metal Physics, Urals Division of Russian Academy of Sciences, 620219 Ekaterinburg, Russia

(Received 28 August 1991; revised manuscript received 16 March 1992)

The temperature dependence of volume diffusion coefficients of the ^{57}Co tracer in single crystals of tungsten has been measured in the temperature range 1680–2270 K by a sectioning method of high depth resolution based on anodic oxidation of the specimen. The temperature dependence parameters are $D_0 = 0.16_{-0.08}^{+0.17} \text{ cm}^2 \text{ s}^{-1}$ and $Q = 118.7 \pm 2.7 \text{ kcal/mole}$. An analysis of our data shows that the diffusion of cobalt in single crystals of tungsten is “normal” and obeys the same regularities as diffusion of tungsten-series impurities in tungsten, for which the diffusion mechanism by monovacancies is well established [N. K. Archipova *et al.*, Phys. Rev. B **30**, 1788 (1984)]. Systematic errors in the determination of volume diffusion coefficients have been discussed. They arise when (i) one uses a low-resolution sectioning method and (ii) one does not take into account the complexity of diffusion fluxes occurring near the external surface of real crystals.

I. INTRODUCTION

During the course of an investigation of the diffusion of homovalent impurities of molybdenum and chromium in single crystals of tungsten,¹ we found that the difference in enthalpies of activation for impurity diffusion (Q_2) and self-diffusion^{2,3} (Q_1) can be described by the Lazarus–Le Claire model,⁴ which accounts for the Coulomb interaction between screened point charges of the impurity (Z_2) and the vacancy ($-Z_1$). Besides that, we also know about the “fast” diffusion of 3d-transition impurities Fe and Co in tungsten.^{5,6} For chromium,¹ the value of $(Q_2 - Q_1)/Q_1$ is about 0.1, and for Fe and Co—according to Refs. 5 and 6—it is 0.3, which exceeds the limits of the empirically established criteria^{7,8} for the vacancy mechanism of diffusion. Since the parameters of volume diffusion of Cr in W are in agreement with the vacancy mechanism of diffusion, it was of interest to elucidate the causes of such a considerable difference in the behavior of two different 3d-transition-metal impurities. Cobalt was chosen as diffusant for the following reasons: (i) in Ref. 6 it was reported that quite complex unexpected changes take place in the coefficients of volume diffusion of cobalt in tungsten with temperature, (ii) the radioactive tracer ^{57}Co having a high specific activity ($\sim 10^4 \text{ Ci/g}$) was commercially available, (iii) our laboratory is engaged in investigations of the regularity of grain-boundary diffusion of Co in W (Ref. 9) and of the properties of impurity states of Co at grain boundaries in W (Ref. 10), for which purposes we must know the parameters of volume diffusion of Co in W, and (iv) the use of ^{57}Co as an atomic probe opens up possibilities for obtaining spectral information for the states in which the ^{57}Co is found as a result of volume diffusion in single crystals of tungsten.

II. EXPERIMENTAL TECHNIQUES AND MATERIALS

The tungsten single crystals to be investigated were grown by crucibleless electron-beam zone melting in a

vacuum of 10^{-5} – 10^{-6} Pa. The initial ratio of the residual resistivities of the single crystals was $R_{300 \text{ K}}/R_{4.2 \text{ K}} = 5 \times 10^4$. The specimens were cut from the single crystals in a spark discharge machine. The specimen dimensions were 4–6 mm (height) and 6–10 mm (diameter). The contaminated and deformed subsurface layer was removed by electropolishing to a depth of 300–500 μm . The cutout blanks were fixed in a cartridge and were lapped on a cast iron plate with chromium oxide (grit size 5 μm). The final polishing was effected on a glass plate using diamond paste (grit size 1 μm). Deformed layers due to grinding and polishing were removed by anodic oxidation in an aqueous solution of ammonia. A layer of 10–15 μm thick was removed by anodic oxidation. Finally the specimens were washed in boiling bidistilled water.

At all these stages of preparation, the specimens were monitored for macroscopic defects on the working surface. An optical microscope ($\times 500$) did not reveal any defects such as specks, pits, etc., on the finished specimens. The structure of Laue patterns from the flat surfaces thus prepared did not differ from that of initial single crystals. The contamination of the working surface by impurities and their distribution over the depth following mechanical and chemical treatment were monitored by means of a secondary ion mass—spectrometer IMS-3f (Cameca, France). Subsequently, only those specimens were used in which a 10–20-nm-thick surface layer contained at most 0.1 at. % total substitutional impurities, and the concentration of these impurities at a depth of 100–200 nm was still two orders of magnitude lower.

The carrier-free radioactive isotope ^{57}Co additionally purified by ion-exchange resins was deposited electrolytically onto the working surface of the specimens. The specific activity of the initial ^{57}Co preparation was 10^4 Ci/g ; the activity of the diffusion source on the specimen was 0.1–0.3 mCi. The thickness of the diffusion source thus deposited was estimated to be a fraction of a nm. The specimen with the source was placed in a polycryst-

talline tungsten container, which was either closed with a lid or, in the case of diffusion annealing at temperatures above 1850 K welded in a vacuum of 10^{-3} Pa by an electron beam.

The annealing was carried out in a vacuum furnace with tungsten heaters. The container with the specimens was inserted in a massive thick-walled tungsten cylinder, which served as a model of a black body (for registering temperature with a help of a pyrometer) and simultaneously equalized the furnace temperature gradients. The annealing temperature was maintained to within ± 2 K by an automatic controller. A tungsten-rhenium thermocouple served as a sensor. The temperature was measured by a disappearing-filament pyrometer. To determine the true diffusion annealing temperature account was taken of the absorption of radiation in the optical elements. A reference tungsten strip lamp served as a source for calibrating the pyrometer. The error of determination of the temperature did not exceed 4–6 K, after accounting for the absorption in the glasses windows. The correction for the warming-up time of the specimens, which in these experiments was about 180–650 s, was taken into account when determining the time of diffusion annealing.¹¹ The correction for cooling time was neglected.

The diffusion zone was profiled by the anodic oxidation sectioning technique.¹² This technique ensures a high depth resolution: it allows one to remove layers of a fraction of a nm thickness. Total thickness of the removed layers, preset by a value of d.c. voltage on the anodic bath, in our experiments was in the range of $(0.9-3) \times 10^{-6}$ cm. For the determination of the layer thickness, use was made of a calibration curve made on the basis of direct weight measurements of layers removed from thin-walled tubular tungsten single crystals.¹

A single-channel analyzer having a well-type scintillation NaI(Tl) crystal was used for the measurement of the intensity of radiation of removed layers. The photopeaks of ^{57}Co γ lines with energies 122 and 135 keV were measured. The maximum activity of removed layers was about 10^3 counts/s. The measurement involved 10^5 counts, ensuring a statistical error of 0.3%. The correction for the dead time of the measuring channel was less than 0.14% and was not taken into consideration.

III. RESULTS

Figure 1 shows all the measured concentration profiles for ^{57}Co in W. At the start of the plot the experimental points deviate downwards forming a maximum on the profile. We shall discuss the conditions that could lead to the observed peculiarities of profiles near the diffusion source. It is known¹¹ that some peculiarities, such as those observed by us at the start of the plot, are due to the evaporation of the tracer from the specimen in the course of diffusion. The evaporation of the tracer in our experiments is confirmed experimentally by the presence of radioactive cobalt on the internal sides of containers used for diffusion annealing. Measurements we conducted showed that only about 10% of the total activity deposited on the specimen working surface prior to the an-

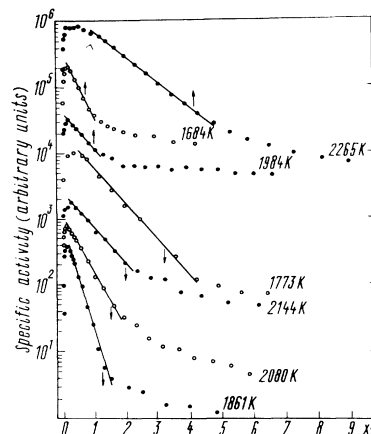


FIG. 1. Coordinate dependencies of concentration of ^{57}Co in W. Each division on the abscissa represents 1×10^{-8} cm² for the 2265-, 2144-, and 2080-K annealings, 1×10^{-9} cm² for the 1984- and 1861-annealings, and 1×10^{-10} cm² for the 1773-K annealing.

nealing was actually found in the diffusion specimen. This corresponded approximately to the ratio of the specimen surface area to the container's internal surface area. Such a relationship could exist only if the deposited activity evaporated from the specimen working surface as the diffusion annealing temperature was attained. Diffusion in this case occurs from a variable gas source whose concentration decreases as a result of natural decrease in the cobalt content in the atmosphere of the container. Evidently, the process of evaporation of cobalt from the diffusion zone begins when the concentration of the tracer in the gas phase becomes lower than that on the specimen surface. Thus one may assume that the profile we obtained corresponds to the diffusion from the variable source and that at a certain instant of time an evaporation process is imposed. Since a part of the experiments (at $T > 1850$ K) took place in welded-up containers, the reduction of cobalt concentration in the container atmosphere was, in this case, determined not by the flow of vapor into the furnace, but by the diffusion of the tracer into the walls of the polycrystalline container.

The following formula was used to calculate the coefficients of volume diffusion:

$$D = (4t\beta)^{-1}, \quad (1)$$

where t is the diffusion annealing time, $\beta = \partial \ln C / \partial x^2$, and C is the tracer concentration at a depth x of the diffusion zone.

Let us estimate the systematic errors that could have been introduced in the course of the determination of the volume diffusion coefficients based on the description of diffusion from instantaneous source into semi-infinite homogeneous specimen. If we had had in our experiments a constant diffusion source, the maximum systematic error resulting from the use of formula (1) would have been about 10%. It is clear that in the case of a variable source the value of the systematic error would be less than that with a constant diffusion source. It will be

shown later on that the discussed error can be considered as a random one for the entire temperature-dependence range of diffusion coefficients. Hence, compared with other errors (large random errors), this error may be disregarded in our experiments.

Now we shall discuss the peculiarities of concentration profiles at the end for the diffusion zone. "Tails," which occur because of diffusion along short-circuiting paths, are formed at the end of profiles. The characteristics of these tails depend little on the diffusion annealing conditions. The following approach is used to calculate coefficients of volume diffusion on the basis of such distorted distributions.

First, the experimental profiles were plotted in $\ln C$ vs $x^{1.2}$ coordinates. In this representation, the profile parts due to diffusion along grain boundaries in a polycrystal or along dislocation walls in a single crystal must be linear. These coordinates were used for graphic extrapolation of the tail into the initial part of the profile and for subtraction of the extrapolated values from experimental points.

Second, as has been noted above, the maxima observed at the start of profile are due to the evaporation of the tracer from the specimen. From the position of the maxima at the start of the profile the vaporization rate can be estimated using the procedure suggested in Ref. 13. We introduced the evaporation correction and obtained corrected values of concentration in the entire diffusion zone. In all cases the evaporation correction did not exceed 20%.

Figure 2 shows the final profiles in the Co diffusion zones in single crystals of tungsten after all the corrections described above have been introduced. Table I presents experimental conditions for diffusion experiments and values of volume diffusion coefficients computed from $\ln C$ vs x^2 straight lines.

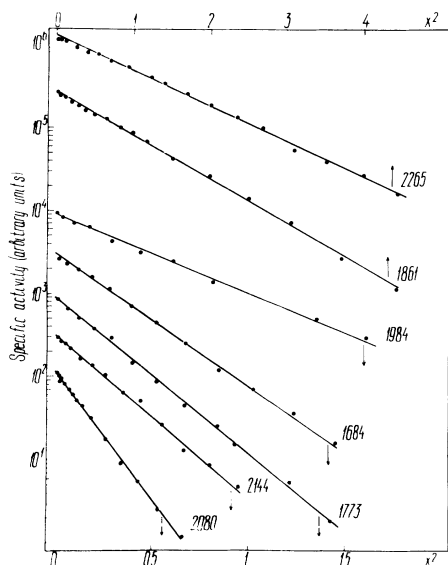


FIG. 2. The corrected coordinate dependencies of the concentration of ^{57}Co in W. Each division on the abscissa represents $1 \times 10^{-8} \text{ cm}^2$ for 2265-, 2144-, and 2080-K annealings, $1 \times 10^{-9} \text{ cm}^2$ for the 1984-K annealing, and $1 \times 10^{-10} \text{ cm}^2$ for the 1861- and 1773-K annealings.

TABLE I. Diffusion of cobalt in tungsten single crystal.

T (K)	$10^4 t$ (s)	D (cm^2s^{-1})	$(Dt)^{0.5}$ (cm)	$\Delta D/D$ (%)
2265	0.4084	6.11×10^{-13}	5×10^{-5}	+8
2144	0.4195	1.30×10^{-13}	2.3×10^{-5}	+2
2080	0.5603	6.03×10^{-14}	1.8×10^{-5}	+11
1984	0.9337	1.23×10^{-14}	1.1×10^{-5}	-9
1861	1.7257	1.49×10^{-15}	5.1×10^{-6}	-20
1773	1.8296	3.23×10^{-16}	2.4×10^{-6}	-14
1684	7.9455	8.24×10^{-17}	2.6×10^{-6}	+30
1573	0.3600	9.56×10^{-16}		
1561	0.6583	3.47×10^{-17}		

With the view of extending the investigation over a wider temperature range for a determination of the volume diffusion coefficients and also where the grain boundary diffusion was measured in this system,⁹ we carried out annealings at 1573 and 1561 K. Figure 3 presents the relevant profiles. The graphs reveal all the peculiarities of profiles obtained at high temperatures. After the corrections described above were made, linear dependence of $\ln C$ vs x^2 was obtained in these profiles too. The values of diffusion coefficients calculated are presented in Table I.

Figure 4 shows an Arrhenius dependence of volume diffusion coefficients of Co in W and a normal deviation plot $\sigma = (D/D_{\text{calc}}) - 1$ corresponding to this relationship. Here D_{calc} is the value calculated from the dependence of $\ln D (T^{-1})$, obtained by the regression analysis and D is the experimental value. The average deviation $\bar{\sigma} = \pm 15\%$, while the normal deviations σ at 1861 and 1684 K were within twice the $\bar{\sigma}$. Therefore, these values were included in the temperature-dependence calculations. The values of diffusion coefficients obtained for 1573 and 1561 K were found to be one and two orders of magnitude higher than the values calculated on the basis of the Arrhenius dependence. Therefore, these values were not included in the calculations of the temperature dependence of volume diffusion coefficients. The causes of such large deviations will be discussed below. The parameters of the temperature dependence of diffusion

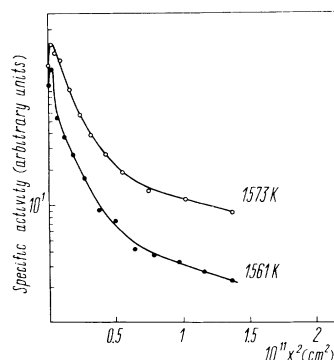


FIG. 3. Coordinate dependencies of concentration of Co in W at 1573- and 1561-K annealings.

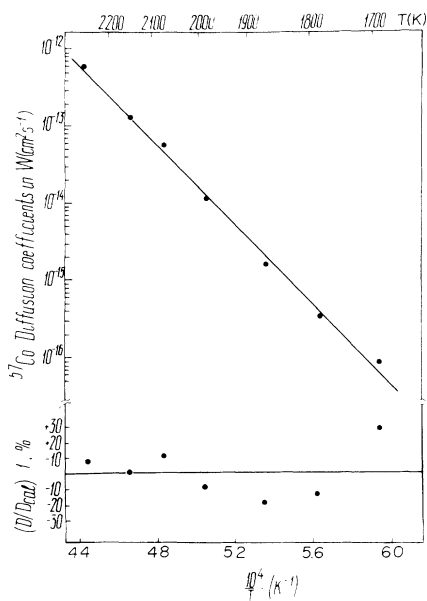


FIG. 4. Temperature dependence of volume diffusion coefficients of Co in single-crystal W and normal deviations of measured D values $\sigma = (D/D_{\text{calc}}) - 1$.

coefficients are as follows:

$$(D_2)_0 = 0.16 \pm_{-0.08}^{+0.17} \text{ cm}^2 \text{ s}^{-1},$$

$$Q_2 = 118.7 \pm 2.7 \text{ kcal/mole}.$$

IV. DISCUSSION OF RESULTS

We shall now compare our results with those of Lee, Klockgeter, and Herzig⁶ for volume diffusion of Co in single crystals of W. Figure 5 shows the temperature dependence of coefficients of diffusion of Co in W from Ref. 6. The plot is a curve having its convex part turned upwards. The straight line of $\ln D(T^{-1})$ plotted using our data (solid line) is given for comparison. The dashed line is the temperature dependence of self-diffusion coefficients from Refs. 2 and 3. It is evident that diffusion coefficients in the common temperature range measured in Ref. 6 exceed our values by two to three orders of magnitude. In order to determine the causes of such a substantial discrepancy we must note that in both experiments (see Fig. 1) the concentration profiles had a complex shape. In both cases profiles had tails. In our experiments there was also evaporation of the tracer. In such situations, when the temperatures of the experiments are sufficiently low and the short-circuiting effects are rather large, an additional analysis to deduct the contribution of the diffusion in short-circuiting paths in the diffusion profiles is needed. Let us examine a typical profile, which was obtained on the basis of experiments involving single crystals or polycrystals at relatively low temperatures.

It has been shown for some time¹⁴ that there exist complex profiles, which under favorable conditions exhibit three characteristic parts. Figure 6 displays a profile from Ref. 14 for ^{95}Nb in polycrystalline W following diffusion annealing at 1672 K ($0.45T_{\text{melt}}$) for 8 h; here

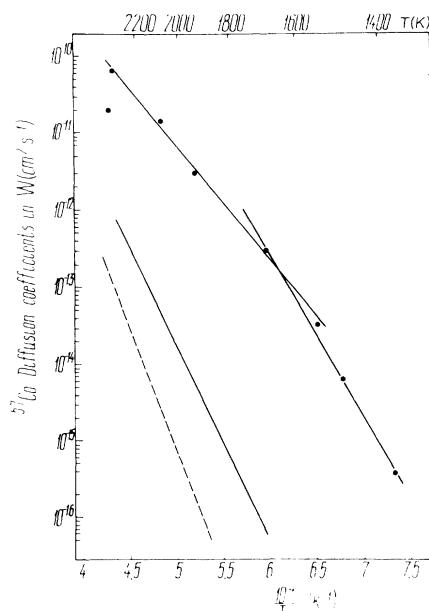


FIG. 5. Temperature dependence of volume diffusion coefficients of Co in W from Ref. 6 (solid points), this work (solid line), and self-diffusion data from Refs. 2 and 3.

T_{melt} is melting point. This profile was obtained by sectioning the diffusion zone into layers by means of anodic oxidation. The first 15 nm were removed layer by layer each 1.5 nm thick. Then the thickness of removed layers was increased to 8 nm (second zone part from 15 to 150 nm). Finally the remaining part of the zone was sectioned into layers each 30 nm thick. Using such a high-resolution analytical method, it became possible to obtain a profile (Fig. 6) having three parts.

Part 1 features Gaussian distribution of concentration and a concentration drop of two to three orders of magnitude, directly adjoining the diffusion source. The authors of Ref. 14 stress that at relatively low temperatures part 1 can be detected, if it exists, only by using the high-

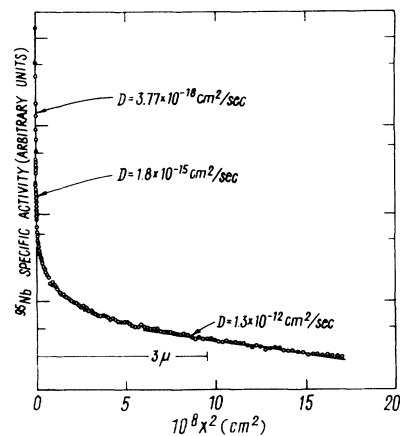


FIG. 6. Coordinate dependence of concentration of ^{95}Nb in polycrystalline W.

TABLE II. Diffusion coefficients of ^{95}Nb in tungsten and ^{195}Au in gold.

System	Ref.	T (K)	D_{vol} (cm^2s^{-1}) extrapolated from	Calculated D values from different parts of the profile	
				Part 1	Part 2
^{95}Nb in polycryst. W	14	1672	3.2×10^{-18a}	3.8×10^{-18}	1.8×10^{-15}
^{95}Au in single-cryst. Au films	15	652	1.88×10^{-16}		8.3×10^{-16}
		598	4.1×10^{-17}		2.2×10^{-16}
		568	6.3×10^{-18b}		3.8×10^{-17}
		548	1.6×10^{-18}		1.0×10^{-17}
		520	2.1×10^{-19}		1.4×10^{-18}

^aReference 14.^bReference 21.

resolution method of sectioning of the diffusion zone into layers. As Table II shows, the initial part 1 with a depth of up to 15 nm yields a correct value of volume diffusion coefficient in good agreement with a value extrapolated from high temperature and measured on single crystal. When a profile of the type shown in Fig. 6 is formed, a correct value of volume diffusion coefficient can be obtained through the use of an analytical method for which the following relationship holds true:¹¹

$$\Delta x \leq 0.25(D_{\text{vol}}t)^{0.5}, \quad (2)$$

where Δx is the thickness of the removed layer.

Part 2, sometimes directly adjoins part 1 or, as will be shown below, sometimes approaches the diffusion source. Part 2 also features a Gaussian distribution, but the concentration drop is only one to two orders of magnitude. Table II gives the following value of diffusion coefficient: $D_{\text{eff}} = (10^1 - 10^3)D_{\text{vol}}$, determined from the slope of part 2 (depth within 15–150 nm).

In the case where part 2 directly adjoins the diffusion source, as it was in the investigation of self-diffusion in an epitaxial single-crystal gold film¹⁵ (Fig. 7), the origin of this part 2 is beyond doubt. Indeed, epitaxial single-

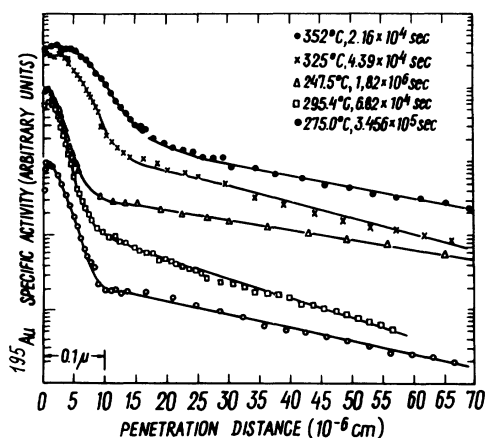


FIG. 7. Coordinate dependencies of concentration of ^{195}Au in single-crystal Au films.

crystal films contained a dislocation density of $N = 10^{12} - 10^{13} \text{ cm}^{-2}$. Therefore, in these experiments the following condition is fulfilled:

$$L \leq (D_{\text{vol}}t)^{0.5}, \quad (3)$$

where L is the distance between dislocations in the film on these zone parts. Self-diffusion in such conditions was carried out in the Hart regime,¹⁶ and the diffusion coefficient for this quasi-uniform part of the specimen determined from Gaussian concentration distribution is

$$D_{\text{eff}} = D_{\text{vol}}(1 + fD_{\text{disl}}) \quad (4)$$

where f is the volume fraction of dislocations in the sample volume of the localization of profile part 2, D_{disl} is the diffusion coefficient along dislocations (if for the common case there is confidence that the diffusion properties of this near surface layer have not changed due to another cause, for example, as a result of strong doping). Under such conditions there was simply no part 1 in Ref. 15. Naturally, it was not observed when the diffusion zone was sectioned into layers by sputtering in argon plasma with a resolution of 3 nm. Diffusion coefficients calculated in accordance with the Gaussian profile (Table II) were found to be 4–8 times higher than the values extrapolated into this temperature range according to $\ln D(T^{-1})$ measured at high temperatures on bulk single crystals (having dislocation densities only of the order of $10^5 - 10^7 \text{ cm}^{-2}$).¹⁴

Similar results were obtained in the investigation¹⁷ on self-diffusion in $\alpha\text{-Fe}$. Using the criterion of the authors in Ref. 17, the diffusion zone was related to dislocation density as

$$(D_{\text{vol}}t)^{0.5} \leq (\pi N)^{-0.5}, \quad (5)$$

where N is the dislocation density. The method of sputtering in argon plasma with a resolution of 1.5 nm was used to determine diffusion coefficients from Gaussian distribution. Their values were found to be several times smaller compared to those determined by other authors, where criterion (5) was not fulfilled (see Ref. 17). However, when the depth of the diffusion zone was increased to $(D_{\text{vol}}t)^{0.5} \approx 30 - 100 \mu\text{m}$ in the same specimens with a dislocation density $N = 10 \text{ cm}^{-2}$; the profile still

remained Gaussian. The diffusion coefficient determined was 1.5–2 times higher than from the shortest profile.

Let us now return to the diffusion coefficients obtained at 1578 and 1561 K. Apparently in the initial part of our profile we also have a part 2. Since these two diffusion zones are smaller than 50 nm, the structural defects in such a thin surface layer can differ considerably from those in the single-crystal volume, as a result of incomplete removal of the residual near the surface defects.

Part 3 of the profile located to large depth of the diffusion zone is called a "tail." Its characteristic is non-Gaussian distribution of concentration, since for a diffusion along isolated dislocations we have $\ln C(x)$, while for a diffusion along dislocation walls or grain boundaries we have $\ln C(x^{1/2})$ are linear dependencies.¹⁸ In part 3 of the profile a drop in concentration, as a rule, does not exceed 1–1.5 orders of magnitude. It is the main source of information on diffusion properties of regions in which the accelerated diffusion is localized. It is the usual practice in investigations of volume diffusion to use part 3 of the profile to extrapolate concentration in the region of the diffusion zone, adjoining the diffusion source, to subtract this contribution, and to calculate "correct" values of "volume" diffusion coefficients. However, as has been shown above, the properties of part 2 of the profile, if it is present, render such a procedure useless, as noted in Ref. 9, where investigation of the diffusion of ⁵⁷Co on tungsten polycrystals is made, and as in the example given above of two profiles measured after 1561- and 1573-K annealings.

Thus, (i) the analysis of the peculiarities of profiles created at relatively low temperatures in single-crystal and polycrystalline specimens and (ii) the comparison of these peculiarities with the structure of specimens and resolution of the sectioning method allow us to comment on the investigation in Ref. 6 that the authors used: Tungsten single crystals, the surface layers of which apparently had a high defect density, so that no part 1 of the profile existed in the concentration profile, and a grinding sectioning method for profiling the diffusion zone, which has lower resolution. This did not allow the authors of Ref. 6 to detect, even if they existed, volume diffusion zones with parameters $(D_{\text{vol}}t)^{0.5} = (0.8-50) \times 10^{-6}$ cm characteristic of the system under examination in the temperature range of the study. Hence, there are no grounds to invoke special diffusion mechanisms for 3d-transition-metal impurities in tungsten, inasmuch as unexpectedly high values of diffusion coefficients of Co in tungsten single crystals measured in Ref. 6 are incorrect.

In view of the above, it is evidently of interest to analyze again the results of investigations of self-diffusion in "normal" metals, wherein a slightly curved Arrhenius dependence of self-diffusion coefficients was established. This dependence arose as a result of the emergence of increased values of diffusion coefficients at low temperatures. The considerations presented above may help us understand these results.

Now it remains only to discuss whether one can draw a definite conclusion on the diffusion mechanism in this system. For this we shall use the concepts presented in

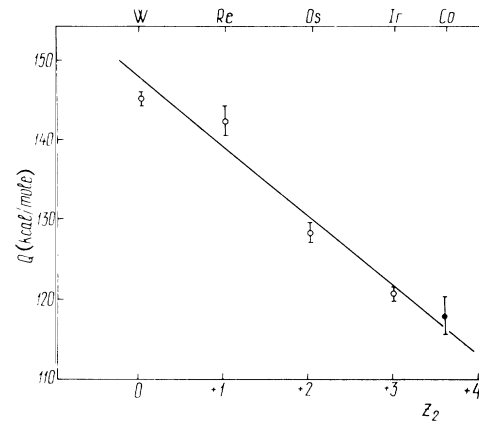


FIG. 8. Dependence of activation enthalpies Q_2 for diffusion of tungsten-series impurities in tungsten single crystals on excess charge Z_2 of these impurities.

our earlier paper.² Figure 8 shows a plot of activation enthalpies for diffusion of a series of impurities in W vs Z_2 , the excess charge of these impurities. A somewhat arbitrary assumption was used here: that, as for solvents of group I noble metals, the excess charge of the tungsten-series impurity is simply equal to the difference of valences of impurity and matrix. Then, within the framework of the Lazarus–Le Claire vacancy diffusion mechanism model⁴ one should expect a practically linear dependence of Q_2 on Z_2 .

As Fig. 8 shows, this dependence is observed for impurities of the tungsten series. We shall use this dependence to draw a conclusion on the mechanism of Co diffusion in W. We shall assume that if the parameters of the diffusion of Co in W agree with this dependence, then diffusion of Co in W takes place by the vacancy mechanism. It is apparent that to check this assumption one must determine more or less correctly the excess charge of Co in W. The effective potential of this 3d-transition-metal impurity can substantially differ from those of the tungsten series impurities. For an independent deter-

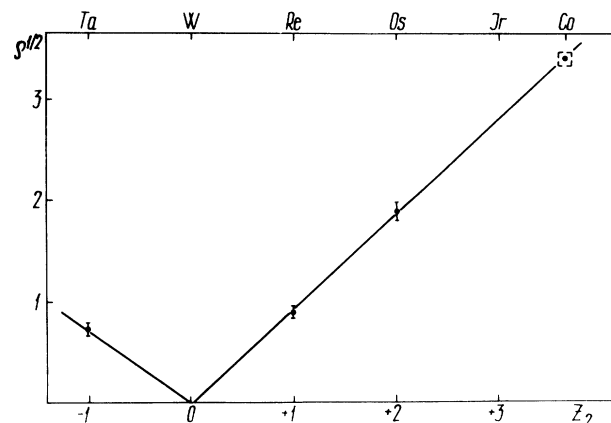


FIG. 9. Dependence of residual resistances of impurities on excess charge.

mination of the effective charge of Co in W, we shall use empirical relationships of the residual resistances of relevant impurities in solid solutions.^{19,20} Fortunately, such data are available for our systems (see Fig. 9). The value of $\rho^{0.5}(\text{Co})$ corresponds to $Z_2(\text{Co})=3.6\pm 0.2$, this being above $Z_2(\text{Ir})=3$, in full accordance with increase of the positive effective charge on the small radius homovalent impurity site owing to the environment relaxation. As is evident from Fig. 8, the experimental value of diffusion activation enthalpy $Q_2(\text{Co})=118\pm 2.7$ kcal/mole is in good agreement with the dependence $Q_2(Z_2)$ for impurities in tungsten. A similar relationship holds true also for $\ln(D_2)_0$ vs Z_2 (Fig. 10), where $(D_2)_0$ is the preexponential factor for impurity diffusion. Thus, one can conclude with sufficient confidence that the mechanism of diffusion of Co in W does not differ from those of self-diffusion and heterodiffusion of tungsten-series impurities.

One can expect that other 3d-impurities are not fast diffusing at least in a matrix of group-VIB atoms. However, for the final solution of this problem we hope to carry out an investigation of the diffusion of manganese and technetium in tungsten.

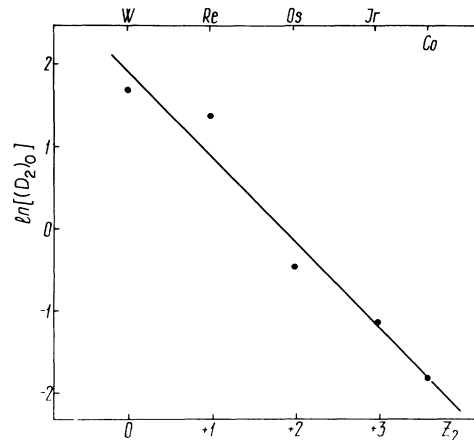


FIG. 10. Dependence of $\ln(D_2)_0$ on excess charge Z_2 .

ACKNOWLEDGMENTS

The authors wish to express their gratitude to S. V. Vonsovsky for his constant support, and I. P. Polikarpova, G. N. Tatarinova, S. N. Matveev, and V. M. Koloskov for technical assistance.

¹S. M. Klotsman, V. M. Koloskov, S. V. Osetrov, I. P. Polikarpova, G. N. Tatarinova, and A. N. Timofeev, *Fiz. Metal. Metalloved.* **67**, 767 (1989).

²N. K. Archipova, S. M. Klotsman, I. P. Polikarpova, G. N. Tatarinova, A. N. Timofeev, and L. M. Veretennikov, *Phys. Rev. B* **30**, 1788 (1984).

³J. N. Mundy, S. J. Rothman, N. Q. Lam, H. A. Hoff, and L. J. Nowicki, *Phys. Rev. B* **18**, 6566 (1978).

⁴A. D. Le Claire, *Philos. Mag.* **7**, 141 (1962).

⁵A. A. Bugai, V. E. Kosenko, and E. G. Miselyuk, *Zh. Techn. Fiz.* **27**, 207 (1957).

⁶J. S. Lee, K. Klockgeter, and Ch. Herzig, *J. Phys. (Paris) Colloq.* **51**, C1-569 (1990).

⁷N. L. Peterson, *J. Nucl. Mater.* **69-70**, 3 (1978).

⁸S. M. Klotsman, *Fiz. Metall. Metalloved.* **55**, 297 (1983).

⁹N. K. Archipova, V. N. Kaigorodov, S. M. Klotsman, and E. V. Kozevina, *Fiz. Metal. Metalloved.* **N3**, 132 (1991).

¹⁰S. M. Klotsman, *Usp. Fiz. Nauk.* **160-162**, 99 (1990) [*Sov.*

Phys. Usp. **33**, 55 (1990)].

¹¹R. E. Pawel and T. S. Lundy, *J. Electrochem. Soc.* **115**, 233 (1968).

¹²S. J. Rothman, *Diffusion in Crystalline Solids*, edited by G. E. Murch and A. S. Nowick (Academic, New York, 1984).

¹³I. Sh. Trachtenberg, *Fiz. Metal. Metalloved.* **37**, 348 (1974).

¹⁴T. S. Lundy and R. E. Pawel, *Trans. Metal. Soc. AIME* **245**, 283 (1969).

¹⁵D. Gupta, *Phys. Rev. B* **7**, 586 (1973).

¹⁶E. Hart, *Acta Metal.* **5**, 597 (1957).

¹⁷Y. Iijima, K. Kimura, and K. Hirano, *Acta Metal.* **36**, 2811 (1988).

¹⁸A. D. Le Claire and A. Rabinovitch, *J. Phys. C* **15**, 3455 (1982).

¹⁹L. Uray, *J. Phys. F* **17**, 1013 (1987).

²⁰B. N. Aleksandrov, *Fiz. Nizkich. Temper.* **12**, 392 (1986).

²¹S. M. Makin, A. M. Rowe, and A. D. Le Claire, *Proc. Phys. Soc. London* **70**, 545 (1957).